Spin-Torque Oscillator using a Perpendicular Polarizer with Double Free Layers

Soo-Man Seo and Kyung-Jin Lee*

Department of Materials Science and Engineering, Korea University, Seoul 136-713, Korea

We conducted a micromagnetic modeling study to investigate the spin torque oscillator (STO) using a perpendicular polarizer. We used an additional layer of negative anisotropy constant materials (NAM) on a conventional STO. For the NAM layer, the magnetic easy plane is parallel to the in-plane easy axis of the free layer, and inhibits the development of the out-of-plane component of the magnetization in the free layer. As a result, this new type of STO provides a high frequency limit up to 50 GHz.

Keywords : spin transfer torque, spin torque oscillator, anisotropy energy, negative anisotropy

1. Introduction

The spin transfer torque (STT) [1] caused by the transfer of the spin angular momentum from the spin-polarized conduction electron to the local magnetization has attracted much attention in terms of its application and fundamental physics [2, 3]. In the magnetic multi-layer system, the STT acts similarly to an anti-damping torque on the magnetization and excites spin waves [4], which leads to current-induced magnetic switching [5].

When the intrinsic damping torque is compensated by STT, the local magnetization can sustain its precession motion. This steady motion of the magnetization provides a new method for applications of spintronic devices. One possible application is the wide-band tunable radio frequency (RF) oscillator for the application of telecommunication or logic devices, *i.e.* so-called spin torque oscillators (STO). From theory [6] and experiments [7], the current-induced precession can be achieved even without an external field by using the perpendicular polarizer as a pinned layer. Another example is the microwave assisted magnetic recording [8]. This concept requires several tens of GHz to gain the saturation digital recording at fields significantly below the medium coercivity. This is because the frequency of the ac field generated by the STO should be about the Larmor frequency, which is proportional to the coercivity of the medium. For instance, for a medium with a coercivity (or

the anisotropy field) of about 2 T, the needed frequency is 50 GHz.

According to the theoretical work [6], the angle between the precessing magnetization and the precession axis becomes smaller as the current (*i.e.* STT from the perpendicular pinned layer) increases. Therefore, the highest frequency obtained in this structure is determined by the current which provides the out-of-plane saturation of the magnetization in the free layer (*i.e.* the tiling angle with respect to the effective field = 0). Since a higher frequency is better for the microwave assisted recording, this fundamental limitation should be resolved. In this work, we introduce negative anisotropy materials (NAM) for the high frequency excitation. The magnetic anisotropy energy is defined as follows,

$$E_K = K \sin^2 \theta \qquad (1)$$

where θ is the angle between the local magnetization and the magnetic easy axis. For the conventional design of STO, the easy magnetization axes of the free layer lie on the film plane (xy-plane of Fig. 1). From the definition of the anisotropy energy (Eq. (1)), for a negative K value, the anisotropy energy (E_K^{NAM}) of the NAM layer should be minimized (maximized) for $\theta = 0°$ (90°). Thus, the magnetization ($\vec{M}^{NAM}$) of the NAM layer energetically prefers to sustain its direction within the xy-plane. Also, it can be expected that $\vec{M}^{NAM}$ oscillates along the z-axis, since E_K^{NAM} is independent of the in-plane angle. Several NAMs have previously been experimentally reported, e.g. CoFe, α-FeC, NiAs-typed MnSb, and hcp CoIr [9-12]. To explore the STO with NAM layer, we performed a micro-

*Corresponding author: Tel: +82-2-3290-3289
Fax: +82-2-928-3584, e-mail: kj_lee@korea.ac.kr
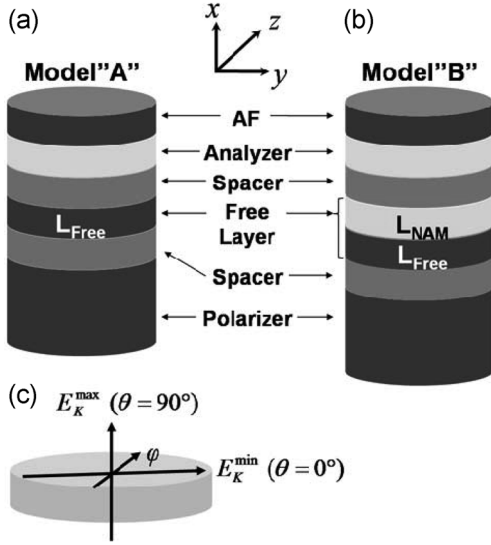
Fig. 1. Schematic diagram of modeling system. (a) Conventional STO, (b) STO with negative anisotropy materials (NAM) layer. (c) Angle dependence of anisotropy energy of magnetization with negative anisotropy constant. Here, θ and φ correspond to the out-of-plane and in-plane angle, respectively.

magnetic simulation. In a comparison of the excited frequency of STO with and without the NAM layer, the current-driven precession frequency is obtained up to 50 GHz.

2. Micromagnetic Modeling

To describe the effect of STT, the modified Landau-Lifshitz-Gilbert equation including additional torque terms is used,

$$\frac{\partial \mathbf{M}}{\partial t} = -\gamma \mathbf{M} \times \mathbf{H}_{eff} + \frac{\alpha}{M_S} \mathbf{M} \times \frac{\partial \mathbf{M}}{\partial t} - \frac{\gamma a_J}{M_S} \mathbf{M} \times (\mathbf{M} \times \hat{p})$$

$$- \frac{b_J}{M_S^2} \mathbf{M} \times \left(\mathbf{M} \times \frac{\partial \mathbf{M}}{\partial x} \right) \quad (2)$$

where $\mathbf{M}$ is the local magnetization vector, γ is the gyromagnetic ratio ($= 1.76 \times 10^7$ sec^{-1}Oe^{-1}), $\mathbf{H}_{eff}$ is the effective field consisting of the anisotropy, exchange, magnetostatic, and external field, M_S is the saturation magnetization and α is the Gilbert damping constant. The coefficients a_J and b_J are given by $\hbar \eta j_e / 2eM_S d$ and $Pj_e \mu_B / eM_S$, respectively, where η is the spin polarization coefficient, j_e is the electrical current density, e is the electron's electric charge, P is the spin polarization, d is the thickness of the free layer, and $\hat{p}$ is a unit vector along the direction of the magnetization of the pinned layer. Here, a_J and b_J represent the magnitude of the in-plane torque

and the adiabatic spin torque (not the perpendicular torque or field like torque), respectively. The temperature is assumed to be zero. Fig. 1 shows a schematic diagram of the STO with the single free layer (L_{Free}) (Model "A") and double free layers consisting of a conventional soft-magnetic free layer and the NAM layer (Model "B"). Since the effect of STT appears on L_{Free} and L_{NAM}, we considered the magnetization dynamics in these two layers. The nanopillar has a circular cross-section with the lateral dimensions of 35×35 nm^2 and the thickness of each free layer (L_{Free} and L_{NAM}) is 10 nm. The unit cell of $35 \times 35 \times 1$ nm^3 is considered (*i.e.*, the free layer consists of 10 cells along the thickness direction). Note that Slonczweiski's ST (a_J torque) is typically subjected on the bottom magnetization of the free layer. Since the a_J torque is only applied on the bottom cell attached to the metallic spacer, there is a distribution of magnetization along the thickness direction in the free layer. Thus, it is reasonable to consider the b_J torque induced by a gradient magnetization ($\nabla \mathbf{M}$), with the exception of the bottom cell of the free layer. We considered the typical soft ferro-magnet for the conventional free layer. Co$_{1-x}$Ir$_x$ ($x = 0.2\sim$ 0.3) is selected for the negative anisotropy materials [11]. The following materials parameters of L_{Free} (L_{NAM}) are used: 1000 (1600) emu/cm^3 for M_S; 0 (-1×10^7) for K; 1.3×10^6 (1.3×10^6) erg/cm for A_{ex}; 0.01 (0.05) for α; 0.7 (0.2) for P; and 0.7 (0) for η.

3. Results and Discussion

The excited frequency (f) and the normalized magnetization (M_N) as a function of current density (j_e) are shown in Fig. 2(a) and Fig. 2(b), respectively. The solid
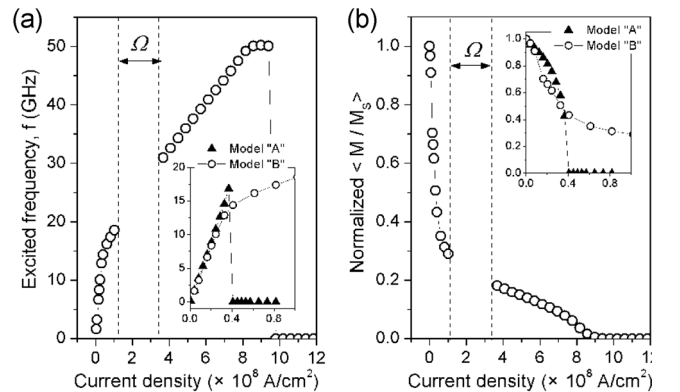
Fig. 2. (a) Excited frequency and (b) normalized magnetization as a function of current density. The solid triangle and open circle correspond to Model "A" and "B", respectively. For Model "B", Ω indicates the region where the eigen frequency does not appear.
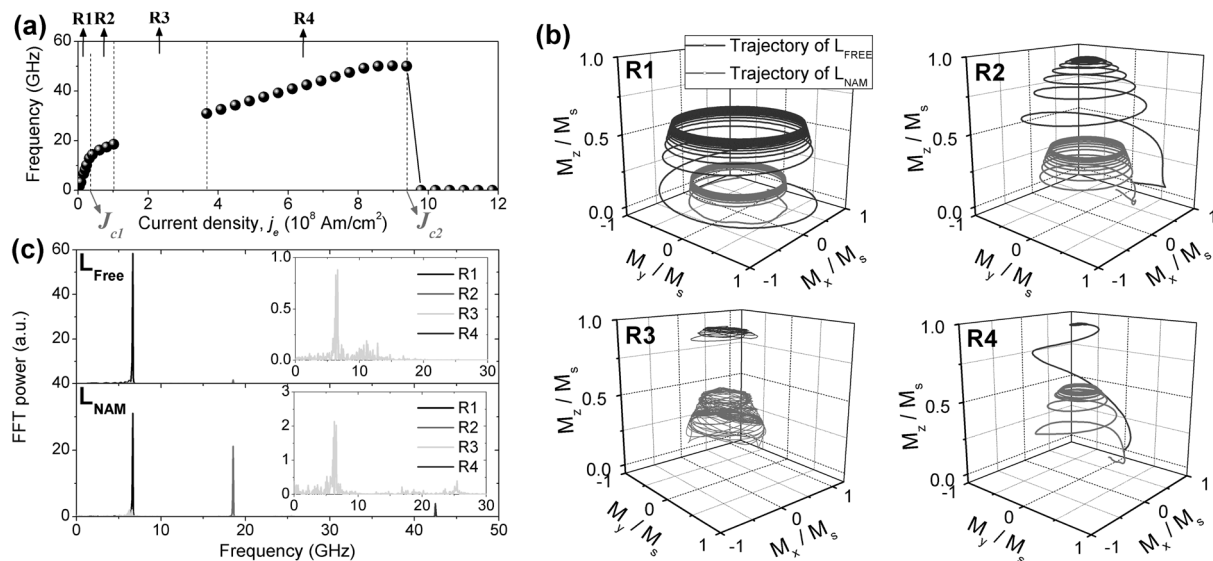
Fig. 3. (a) Excited frequency as a function of current density for model "B". Here, J_{c1} and J_{c2} indicate the critical current density for the saturation of L_{Free} and L_{NAM}, respectively. (b) The typical trajectory of precession motion for R1~R4 is denoted in Fig. 3(a). Blue and red lines indicate the trajectory of the magnetization of L_{Free} and L_{NAM}, respectively. (c) Fast Fourier transform (FFT) spectra of R1~R4. Especially, insets correspond to the case of R2.

triangle and open circle correspond to Model "A" and "B", respectively. As was theoretically predicted [4], the linear relationship between f and j_e is shown for model "A". For $j_e = 4 \times 10^7$ A/cm^2 $(= J_{c1})$, a maximum f (f^{max}) of 16.8 GHz is obtained and $M_N = 0$ (Inset of Fig. 2(b)). Above this critical j_e (j_c), the magnetization of the free layer is saturated at the z-axis and therefore no more precession is achieved at above the f^{max}.

For model "B", below J_{c1}, the relationship between f and j_e is similar to that of model "A" (Inset of Fig. 2(b)). We can then see a reduced slope from J_{c1} and J_{c2} (9.38 × 10^8 A/cm^2). At J_{c2}, f^{max} is 50.3 GHz, which is three times larger than f^{max} model "A". In particular, in the range of j_e = 1~3.6 × 10^8 A/cm^2 (denoted as Ω), there is no eigen frequency for the precession motion.

In order to gain a further understanding of the various excited modes of model "B", we investigated the trajectory of the precession motion. Fig. 3(a) shows the excited frequency as a function of current density for model "B". J_{c1} and J_{c2} indicate the critical current density for the saturation of L_{Free} and L_{NAM}, respectively. According to the dependence between f and j_e, the typical trajectory of the precession motion is observed (Fig. 3(b)). In Fig. 3(b), the trajectories of L_{Free} and L_{NAM} are shown. First, in the range of $0 \sim J_{c1}$ ("R1" in Fig. 3(b)), it is observed that L_{Free} and L_{NAM} coherently precess. From the fast Fourier transform (FFT) spectra of the magnetizations in this range of the current, we can see the single peak (black line peak in Fig. 3(c)). The normalized z-compo-

nent (M_Z/M_S) of L_{Free} is larger than L_{NAM}, since the a_J torque only exerts on the bottom layer of L_{Free}. Second, in the range of $J_{c1} \sim 1 \times 10^8$ A/cm^2, the slopes of f and j_e are reduced. For this range of the current density, we can see that L_{Free} is entirely saturated ("R2" in Fig. 3(b)). From the FFT spectra (red line in Fig. 3(c)), the peak of L_{Free} is close to zero, but the peak of L_{NAM} shows a nonzero value. For the range of $1 \sim 3.6 \times 10^8$ A/cm^2 ("R3" in Fig. 3(b)), the two layers incoherently rotate. Widely distributed FFT spectra were shown (Insets of Fig. 3(c)). For the range of $3.6 \times 10^8 \sim J_{c2}$ ("R4" in Fig. 3), the behavior of the two layers is similar to the case of R2. In both cases of R2 and R4, the excited frequency is entirely a result of the precession of the magnetization of L_{NAM}, since the magnetization of L_{Free} is almost saturated towards the direction of the effective field (z-axis). However, for the case of "R4", the magnetization of L_{Free} is more rapidly saturated in the z-axis, and the tilting angle of L_{NAM} is larger than the case of "R2". Above J_{c2}, the magnetization of the two layers is entirely saturated, and there is therefore no precessional motion of the magnetization.

4. Conclusion

In conclusion, we have investigated the STO using a perpendicular polarizer. We showed the enhanced frequency for the STO with NAM layers. Since the magnetization of the NAM layer prefers an in-plane direction due to the negative anisotropy constant, the NAM layer acts

similarly to an energy barrier for the out-of-plane saturation of L_{Free}. As a result, by inserting a NAM free layer, the critical current density for the saturation of L_{Free} and the oscillation frequency are enhanced. Our results indicate that it is possible to increase the precession frequency by introducing the NAM since it inhibits the out-of-plane saturation of the magnetization in the free layer. This high precession frequency can be used for the STO in the microwave assisted magnetic recording even without heating the medium.

Acknowledgements

References

[1] J. C. Slonczewski, J. Magn. Magn. Mater. **159**, L1 (1996); L. Berger, Phys. Rev. B **54**, 9353 (1996).

[2] S. I. Kiselev et al., Nature **425**, 380 (2003).

[3] S.-W. Jung, and H.-W. Lee, J. Magnetics **12**(2), 1 (2007).

[4] Joo-Von Kim et al., J. Magnetics **12**(2), 53 (2007).

[5] E. B. Myers et al., Science **285**, 867 (1999).

[6] K.-J. Lee, O. Redon, and B. Dieny, Appl. Phys. Lett. **86**, 022505 (2005).

[7] D. Houssameddine et al., Nat. Mater. **6**, 447 (2007).

[8] J.-G. Zhu, X. Zhu, and Y. Tang, IEEE Trans. Magn. **44**, 125 (2008).

[9] M. Takahashi and S. Kadowaki, J. Phys. Soc. Jpn. **48**, 1391 (1980).

[10] M. Takahashi, Y. Takahashi, and H. Shoji, IEEE Trans. Magn. **37**, 2179 (2001).

[11] N. Kikuchi et al., J. Phys. Condens. Matter **11**, L485 (1999).

[12] T. Oikawa et al., IEEE Trans. Magn. **38**, 1976 (2002).